Small impact of stratospheric dynamics and chemistry on the surface temperature of the Last Glacial Maximum in CESM2(WACCM6ma)

Jiang Zhu[1], Bette L. Otto-Bliesner[1], Esther C. Brady[1], Rolando Garcia[2], Mike Mills[2], Douglas Kinnison[2], Jean-Francois Lamarque[1]

[1]*Climate and Global Dynamics Laboratory, National Center for Atmospheric Research, Boulder, Colorado, USA*

[2]*Atmospheric Chemistry, Observations, and Modeling Laboratory, National Center for Atmospheric Research, Boulder, CO, USA*

Key Points:

- We present coupled LGM simulations using CESM2(WACCM6ma) with a high-top atmosphere and compare them with parallel low-top simulations
- The high-top LGM simulations show weaker stratospheric circulation and substantial ozone changes in the troposphere and lower stratosphere
- The active stratospheric dynamics and chemistry in CESM2(WACCM6ma) cause little change (<5%) in LGM surface and tropospheric temperatures

Plain Language Summary: The Last Glacial Maximum (LGM), the peak of the last ice age occurred about 20,000 years ago, has been frequently used to calculate the Earth's climate sensitivity and to evaluate Earth System Models (ESM). These applications of the LGM climate rely on an accurate understanding of the LGM temperature and its relationship with changes in Earth orbits and the subsequent physical, chemical, and biological interactions in the system. How the stratospheric dynamics and chemistry changes impact the LGM temperature is important but not well studied. Here we address this question using a state-of-the-art ESM that has a capability to explicitly simulate stratospheric dynamics and chemistry. Through a comparison with parallel simulations with the same ESM but without the capability of stratospheric dynamics and chemistry, we conclude that stratospheric dynamics and chemistry exert only a minor impact on the LGM surface temperature (<5%). Our results, if confirmed by the other ESMs, suggest that stratospheric dynamics and chemistry do not directly affect much the glacial-interglacial climate change, and ESMs without a capability of stratospheric dynamics and chemistry are sufficient for climate sensitivity and model evaluation studies using the LGM.

Abstract: Stratospheric dynamics and chemistry can impact the tropospheric climate through changing radiatively active atmospheric constituents and stratosphere-troposphere interactions. The impact of stratospheric dynamics and chemistry on the Last Glacial Maximum (LGM) climate is not well studied and remains an uncertain aspect of glacial-interglacial climate change. Here we perform coupled LGM simulations using the Community Earth System Model version 2 (CESM2), with a high-top atmosphere—the Whole Atmosphere Community Climate Model version 6 with a middle atmosphere chemistry mechanism (WACCM6ma). The CESM2(WACCM6ma) LGM simulations show a weaker stratospheric circulation than the preindustrial, 10–35% less tropospheric ozone and 10–50% more ozone in the lower stratosphere. These stratospheric dynamics and chemistry changes cause slightly colder (by <5%) LGM surface and tropospheric temperatures than parallel simulations using a low-top atmosphere model without active chemistry. The results suggest that stratospheric dynamics and chemistry have little direct effect on the glacial-interglacial climate change.

1. Introduction

The LGM has been a focus of paleoclimate research for several decades because it contains important information on how the Earth's climate system responds to external forcings. Reconstructions of the LGM climate have long been used to calculate equilibrium climate sensitivity (ECS) (e.g., Hansen, Sato, Russell, & Kharecha, 2013; Lorius, Jouzel, Raynaud, Hansen, & Treut, 1990; Tierney et al., 2020) and are found to provide a stronger constraint on the upper bound of ECS than any other lines of evidence (Sherwood et al., 2020). LGM climate also provides a premier opportunity to evaluate Earth System Models (ESMs) (Braconnot et al., 2012) and can be used to inform cloud parameterizations that critically determine many aspects of model behavior (Manabe and Broccoli, 1985; Zhu et al., 2021). For these reasons, simulation of the LGM has been a key component of the Paleoclimate Modelling Intercomparison Project (PMIP) since its first phase (Joussaume & Taylor, 1995).

An accurate understanding of the LGM temperature and the associated forcing-feedback processes is critical for its application in climate sensitivity and climate modeling studies. The most recent estimate of the LGM global mean surface temperature (GMST) is approximately 6 °C colder than the preindustrial (Tierney et al., 2020). The LGM global cooling results from changes in Earth's orbit and multiple dynamical, physical, and biogeochemical feedback processes across a range of timescales. Among these processes, the lower greenhouse gas (GHG) concentrations and the conditions of land ice sheets (and the associated effect on sea level) are better known and have been incorporated into most of the coupled LGM simulations (e.g., Kageyama et al., 2021; Otto-Bliesner et al., 2006). Additional Earth system feedbacks from changes in the biogeophysical and chemical processes (such as vegetation and ozone chemistry) are much more uncertain.

Stratospheric dynamics and chemistry and their impact on the LGM climate are much less studied, although they are known to affect the surface climate through stratosphere-troposphere interactions and radiation changes associated with water vapor, ozone, and stratospheric aerosols (Baldwin & Dunkerton, 2001; Mills et al., 2016; Solomon et al., 2010). Limited by the availability of appropriate climate-chemistry models and the high computing demand of these models, most previous modeling studies used either simple models or complex models in a simplified atmosphere-only configuration (Crutzen & Brühl, 1993; Fu et al., 2020; Hopcroft, Valdes, O'Connor, Kaplan, & Beerling, 2017; Martinerie, Brasseur, & Granier, 1995; Rind, Lerner, McLinden, & Perlwitz, 2009; Wang, Fu, Solomon, White, & Alexander, 2020). For example, Fu et al. (2020) and Wang et al. (2020) performed LGM simulations using a "high-top" atmosphere with prescribed sea-surface temperature (SST) and found a weaker Brewer-Dobson circulation and substantial ozone changes, but how these effects may impact the glacial climate cannot be directly investigated in the atmosphere-only configuration. Noda et al. (2018) reported that interactive chemistry caused approximately 20% less LGM cooling in the Meteorological Research Institute ESM (MRI-ESM1), which, to the best of our knowledge, is the only available LGM climate-chemistry simulation in a fully coupled framework. Given the substantial uncertainties in how stratospheric dynamics and chemistry respond to external forcing and how the climate responds to these dynamical and chemical changes (e.g., Chiodo & Polvani, 2019; Chiodo et al., 2018; Hardiman et al., 2019), paleoclimate modeling studies using different ESMs are needed.

In this study, we present LGM simulations using the fully coupled Community Earth System Model version 2 (CESM2) that has a "high-top" atmosphere and explicitly resolves stratospheric dynamics and chemistry. We evaluate the impact on the LGM surface temperature from the stratospheric dynamics and chemistry by comparing the "high-top" simulation against parallel

CESM2 simulations with a "low-top" atmosphere. Our fully coupled framework provides one of the first direct quantifications of the impact from stratospheric dynamics and chemistry on the LGM surface temperature.

2. Models and experiments

CESM2 is the latest and most comprehensive ESM in the CESM series with state-of-the-art components of the atmosphere, land, ocean, and sea ice (Danabasoglu et al., 2020). CESM2 can be configured to run the atmosphere component model in both "high-top" and "low-top" configurations. The "high-top" configuration uses the Whole Atmosphere Community Climate Model version 6 (WACCM6) with 70 vertical levels, spanning from the surface to 6×10^{-6} hPa (~140 km). The "low-top" configuration uses the Community Atmosphere Model version 6 (CAM6) with 32 levels and a model top at 3.6 hPa (~45 km). In addition to the higher model top and superior stratospheric representation, WACCM6 includes a comprehensive chemical mechanism, an extensive representation of secondary organic aerosols, and a prognostic stratospheric aerosol capability (Danabasoglu et al., 2020; Gettelman et al., 2019). WACCM6 is designed to match CAM6 in CESM2 and uses identical physical parameterizations as CAM6 (except that it adds parameterizations for frontal and convective gravity waves), as well as the same vertical levels from the surface to the ~87-hPa level (Gettelman et al., 2019). CESM2(WACCM6) simulates a very similar present-day climate state and climate sensitivity as CESM2(CAM6) (Danabasoglu et al., 2020; Gettelman et al., 2019). In this study, we use WACCM6 at a horizontal resolution of 1.9° in latitude and 2.5° in longitude and a middle atmosphere chemistry mechanism (ma), which simulates 98 chemical species and 298 chemical reactions and resolves important chemistry and aerosol processes for ozone, polar stratospheric clouds, and stratospheric aerosols (Gettelman et al., 2019).

We use the paleoclimate-calibrated modifications (PaleoCalibr) within CESM2, instead of the standard configuration that has a high ECS and simulates unrealistic past extreme warm and cold climates (Zhu et al., 2022; Zhu et al., 2021; Zhu, Poulsen, & Otto-Bliesner, 2020). PaleoCalibr removes an inappropriate limiter on the cloud ice particle number, reduces the microphysical timestep, and has additional minor parameter tuning (Zhu et al., 2022). PaleoCalibr has a lower ECS than the standard CESM2 (4.0 vs 6.1 °C; calculated using a slab ocean with a ~2° atmosphere model) and simulates realistic LGM and the present-day climates (Zhu et al., 2022).

We perform two pairs of preindustrial (PI) and LGM simulations using the fully coupled CESM2(WACCM6ma) and CESM2(CAM6) with PaleoCalibr modifications (denoted as HghTop and LowTop hereafter), respectively. The HghTop simulations (PI_HghTop and LGM_HghTop) use the same boundary conditions as the LowTop counterparts such that any differences from the LowTop simulations are attributable to the additional stratospheric dynamics and chemistry. The LGM boundary conditions include lower mixing ratios of GHGs (CO_2 = 190 ppmv; CH_4 = 375 ppb; N_2O = 200 ppb) than PI, the presence of land ice sheets and the associated effect on sea level, and the Earth's orbital parameters at 21 ka (thousand years before present) (Table 1). The LowTop simulations (PI_LowTop and LGM_LowTop) are initialized from previous CESM simulations and have reached quasi-equilibrium in surface climate with an average LGM ΔGMST of –6.8°C and a top-of-atmosphere (TOA) radiation imbalance of ~–0.1 W m^{-2} (Zhu et al., 2022). PI_HghTop and LGM_HghTop are initialized from the corresponding LowTop simulations and integrated further for 300 years, with TOA radiation imbalance at the end of the simulation comparable to the LowTop simulations (Table 1; see Text S1 in the Supporting Information for the method to initialize the high-top atmosphere and chemistry for the LGM). Following the PMIP4 protocols

(Kageyama et al., 2021), aerosol emissions and vegetation cover are fixed at the preindustrial values in both LGM_LowTop and LGM_HghTop.

Given the importance of aerosol emissions for atmospheric chemistry and climate, we perform an additional LGM sensitivity simulation with a set of aerosol emissions altered from the preindustrial one (LGM_HghTopA). Following Wang et al. (2020), LGM_HghTopA removes all the anthropogenic components from the preindustrial emissions, scales down the fire CO and NO_x emissions to 10%, and scales down the soil NO_x emissions to 98%. These scaling factors are derived from previous modeling and observational studies (Murray et al., 2014; Power et al., 2008; Wang et al., 2020). NO_x emissions from lightning are interactive in the model. LGM_HghTopA together with LGM_HghTop should bracket a reasonable range of uncertainty in aerosol emissions.

We use the mean age of stratospheric air (AoA) as an indicator to examine the stratospheric circulation change. AoA is the average transport time of an air parcel from its entry point (usually taken to be at the tropical tropopause) into the stratosphere to a given location in the stratosphere (Hall & Plumb, 1994). An increase of AoA indicates a weakening of the stratospheric ventilation and therefore a weaker Brewer-Dobson Circulation. AoA is obtained in the model by comparing the mixing ratio of an "age of air tracer" at a given location in the stratosphere to that at a reference point in the tropical tropopause (0.95°N, 143 hPa). The age of air tracer is inert and has a uniform mixing ratio at the surface that increases linearly with time (Garcia, Marsh, Kinnison, Boville, & Sassi, 2007; Garcia, Randel, & Kinnison, 2011).

3. Results

3.1 Stratospheric age of air increases in the LGM simulations

158 The LGM simulations show a much older AoA than PI, indicating a weaker glacial Brewer-
159 Dobson Circulation. AoA in PI_HghTop ranges from 0.0 years near the tropical tropopause to >3.5
160 years in the high-latitude stratosphere (contours in Figure 1a). In LGM_HghTopA, AoA is older
161 than the PI values by approximately 1.0 year in the equatorial stratosphere and by ~1.0–1.4 years
162 over the higher latitudes (shadings in Figure 1a). AoA increases the most in the upper stratosphere
163 and the extratropical lower stratosphere with maximum centers in the subtropics and the Antarctic.
164 The AoA increases are insensitive to the treatment of LGM aerosol emissions (LGM_HghTopA
165 versus LGM_HghTop; Figure 1b).

166 The older AoA and the associated spatial distribution in our fully coupled LGM simulations
167 are similar to results from the WACCM6 atmosphere-only simulation from Fu et al. (2020) (Figure
168 1a versus 1c, shadings). Given the similarity of the atmosphere models in the two sets of
169 simulations (WACCM6ma in ~2° versus WACCM6 in ~1° horizontal resolution), we suggest that
170 our results share the same causal mechanisms as identified in Fu et al. (2020), i.e., the weaker
171 stratospheric circulation caused by the weaker parameterized and resolved gravity wave drags
172 under glacial conditions. The magnitude of changes is larger by ~0.4–0.6 years in our coupled
173 simulation, likely attributable to the different horizontal resolution and extent of LGM cooling in
174 these simulations (not shown). The older AoA and the weakening of Brewer-Dobson Circulation
175 under the LGM cooling forcing are opposite to the younger AoA and the strengthening of Brewer-
176 Dobson Circulation in future projections in response to the GHG increase, which is explained by
177 the opposite changes in the zonal-mean temperature distribution between warming and cooling
178 and the effect on the subtropical jets and wave activities (Garcia et al., 2007; Garcia & Randel,
179 2008).

180 **3.2 Ozone changes in the LGM simulations**

Compared to PI_HghTop, ozone in LGM_HghTopA increases by 5–50% over the tropical lower stratosphere (~110–30 hPa) and decreases by < 5% above (shadings in Figure 1d). In the Southern Hemisphere (SH) mid-to-high latitudes, ozone increases by 5–25% in the lower stratosphere (~100–300 hPa). In the Northern Hemisphere (NH) mid-to-high latitudes, ozone increases by 5–10% in in the lower stratosphere (~300 hPa). In the troposphere, ozone decreases by 10–35%. Approximately half of the tropospheric ozone decreases in LGM_HghTopA can be attributed to the lower LGM aerosol emissions than in LGM_HghTop (Figure 1e; preindustrial aerosol in LGM_HghTop versus no anthropogenic aerosols, 10% of the preindustrial fire NO_x and CO, and 98% of soil NO_x emissions in LGM_HghTopA). The lower NO_x emissions in LGM_HghTopA decrease the tropospheric ozone by reducing chemical production. The treatment of aerosol emissions has little impact on stratospheric dynamics and ozone chemistry (Figure 1b,f).

The overall pattern of ozone changes in LGM_HghTopA—the increases in the lower stratosphere and decreases elsewhere—is consistent with results in the WACCM6 atmosphere-only simulation from Wang et al. (2020) (Figure 1f) and in a climate-biosphere-chemistry model simulation (Geng et al., 2017; Murray et al., 2014). We suggest that the ozone changes in our coupled LGM simulations share the same set of dynamical and chemical mechanisms as in Wang et al. (2020), including a weaker Brewer-Dobson Circulation and its transport, a lower glacial tropopause height, and a temperature dependent chemical reaction rate (Wang et al., 2020).

3.3 Little impact on LGM surface temperatures from stratospheric dynamics and chemistry

The stratospheric dynamics and chemistry changes have little impact on the LGM GMST in our simulations (Figure 2). ΔGMST is –7.08±0.11 °C (±1 standard deviation; averaged over the last 70 years) in the high-top LGM simulation with altered aerosol emissions (LGM_HghTopA –

PI_HghTop; orange in Figure 2), which is 0.21 °C (~3%) colder than in the low-top counterparts (LGM_LowTop – PI_LowTop; red). LGM_HghTop has nearly identical ΔGMST and TOA radiation imbalance as LGM_ HghTopA (orange versus blue in Figure 2), indicating that the treatment of LGM aerosol emissions has little influence on the glacial surface temperature. Our finding of a small impact from stratospheric dynamics and chemistry is unlikely to be impacted by the equilibrium status of the coupled simulations because they have nearly identical TOA radiation imbalance ($N \approx -0.1$ W m^{-2}; Table 1) and radiative feedbacks of shortwave cloud and surface albedo (not shown).

Stratospheric dynamics and chemistry changes also have little impact on the LGM regional surface temperature. The surface air temperature (SAT) is colder in LGM than PI everywhere, with maximum cooling exceeding 20 °C over the Laurentide Ice Sheet and the polar regions above sea ice (Figure 3a). Differences in the LGM cooling, ΔSAT, between the high-top and low-top simulations (Figure 3c) are in general very small (<~1°C), although some statistically significant differences with values of ~1°C exist above snow and sea ice in the high latitudes, where the surface albedo feedbacks amplify the temperature responses and likely spread the impact to the lower latitudes. The treatment of LGM aerosol emissions has little impact on the SAT with values that are not statistically significantly different over most of the regions between LGM_HghTopA and LGM_HghTop (Figure 3b).

The small climatic impact from the LGM stratospheric dynamics and chemistry extends to the air temperature and water vapor throughout the troposphere (Figure 3d–i). In response to the LGM climate forcing, the simulated tropospheric air temperatures cool by more than 5°C in the tropical lower troposphere and by more than 8°C over the tropical upper troposphere and the high-latitude lower troposphere. The magnitude of the tropospheric cooling differs by less than 1°C

between the high-top and low-top configurations and does not depend on the treatment of LGM aerosol emissions (Figure 3e,f), which are consistent with the small differences in the surface temperature (Figure 3b,c). The tropospheric water vapor decreases by more than 50% over the tropical upper troposphere and over the high-latitude lower troposphere with small differences (< 5% of the preindustrial value) between the high-top and low-top configurations and negligible dependence on the treatment of LGM aerosol emissions (Figure 3d–f).

Compared to the troposphere and the surface, the stratosphere exhibits greater changes due to stratospheric dynamics and chemistry. In response to the reduced radiative cooling from the lowered GHGs, the stratospheric air warms by up to 8°C in the LGM simulations (Figure 3d). The stratospheric warming is much weaker in the NH high latitudes than in the SH, which is attributable to the weaker (resolved) planetary wave drag in the NH and the associated dynamical cooling (Fu et al., 2020). The high-top simulations show greater warming of 1–2°C in the tropical lower stratosphere (Figure 3f), which is consistent with the higher ozone concentration and the lower tropopause. The differences in ΔSAT of up to 1°C in the upper stratosphere (above ~10 hPa) may be artificial and related to the sponge layer in the "low-top" model, which is designed to absorb vertically propagating wave energy and to control the strength of the stratospheric winter jets (Neale et al., 2010). The stratospheric water vapor decreases more (by ~5–20% of the preindustrial values) in the high-top simulations than in the low-top counterparts, mostly over the high latitudes. The additional stratospheric water vapor decreases in the high-top simulations are consistent with the weaker Brewer-Dobson Circulation and the reduced methane oxidation (Wang et al., 2020).

4. Conclusions and Discussion

In this study, we performed a suite of coupled LGM simulations using CESM2(WACCM6ma), which has a high atmosphere model top of ~140 km and a state-of-the-art simulation of stratospheric dynamics and chemistry. Compared to preindustrial conditions, our LGM simulations show an older age of stratospheric air, indicating a weaker Brewer-Dobson Circulation under glacial conditions. Our LGM simulations exhibit ~10–35% less ozone in the troposphere, ~10–50% more ozone in the lower stratosphere over the tropics and the high latitudes of both hemispheres, and slightly less ozone in the middle and upper stratosphere.

The coupled CESM2(WACCM6ma) simulations and the comparison with parallel simulations with a low-top atmosphere (CESM2(CAM6)) enable us to investigate the impact of stratospheric dynamics and chemistry on the glacial climate. We find very minor differences in the surface and tropospheric temperature responses between the high-top and low-top LGM simulations. In the global mean, the high-top LGM simulations produce ~3% more glacial surface cooling than the low-top counterparts. At the regional scale, the high-top LGM simulations cool more by <0.5 ℃ in the low-latitude surface and troposphere and by <1℃ in the high latitudes. The climatic impact from stratospheric dynamics and chemistry shows little dependence on the treatment of LGM aerosol emissions in our simulations.

The small impact of stratospheric dynamics and chemistry on the glacial climate in our CESM2(WACCM6ma) simulations is consistent with their small impact on ECS in CESM2 and its predecessors (Danabasoglu et al., 2020; Marsh, Lamarque, Conley, & Polvani, 2016). Here we quantify ECS to be 4.0±0.1℃ in both CESM2(WACCM6ma) and CESM2(CAM6) in a preindustrial-based $2\times CO_2$ simulations using a slab-ocean model (in the paleoclimate-calibrated configuration (Zhu et al., 2022)). From a radiative forcing and feedback perspective in a low-top modeling framework, our results suggest a small radiative forcing from the glacial-interglacial

changes in ozone and stratospheric water vapor associated with atmospheric chemistry and stratospheric dynamics. Following the approach in Zhu and Poulsen (2021), here we quantify the effective radiative forcing (ERF) from the LGM ozone change to be –0.04 W m^{-2}, which is less than 1% of the total ERF (–5.84 W m^{-2}) in our low-top LGM simulation.

We note that there is a large inter-model spread in the importance of stratospheric dynamics and chemistry in both preindustrial-based and paleoclimate simulations. In preindustrial-based abrupt quadrupling CO_2 simulations, stratospheric ozone chemistry is found to decrease ECS by up to 20% (Nowack et al., 2015), ~7–8% (Dietmüller, Ponater, & Sausen, 2014; Muthers et al., 2014), or ~0% (Marsh et al., 2016). Similarly, the impact on the simulated LGM surface temperature ranges from ~+3% for stratospheric dynamics and chemistry (this study) to ~–20% for the atmospheric chemistry (Noda et al., 2018). The large inter-model spread is likely due to the model dependence in the climate response to chemistry changes, rather than in the chemistry response to forcing (Chiodo & Polvani, 2019; Hardiman et al., 2019; Marsh et al., 2016). Further coordinated paleoclimate simulations using multiple climate-chemistry models are needed to examine the inter-model spread, as well as to investigate the role of stratospheric dynamics and chemistry on the past warm climates, such as the Pliocene and the Early Eocene.

Acknowledgements: The authors thank Jadwiga Richter and Isla Simpson for helpful suggestions on the simulation setup and analysis. The CESM project is supported primarily by the National Science Foundation (NSF). This material is based upon work supported by the National Center for Atmospheric Research, which is a major facility sponsored by the NSF under Cooperative Agreement No. 1852977. Computing and data storage resources, including the Cheyenne

supercomputer (doi:10.5065/D6RX99HX), were provided by the Computational and Information Systems Laboratory (CISL) at NCAR.

Data Availability Statement: CESM2 model code is available at https://doi.org/10.5281/zenodo.3895315. Model simulation data from this study can be accessed through the Earth System Grid Federation.

References:

Baldwin, M. P., & Dunkerton, T. J. (2001). Stratospheric Harbingers of Anomalous Weather Regimes. *Science, 294*(5542), 581-584. doi:doi:10.1126/science.1063315

Braconnot, P., Harrison, S. P., Kageyama, M., Bartlein, P. J., Masson-Delmotte, V., Abe-Ouchi, A., . . . Zhao, Y. (2012). Evaluation of climate models using palaeoclimatic data. *Nature Climate Change, 2*(6), 417-424. doi:10.1038/nclimate1456

Chiodo, G., & Polvani, L. M. (2019). The Response of the Ozone Layer to Quadrupled CO2 Concentrations: Implications for Climate. *Journal of Climate, 32*(22), 7629-7642. doi:10.1175/JCLI-D-19-0086.1

Chiodo, G., Polvani, L. M., Marsh, D. R., Stenke, A., Ball, W., Rozanov, E., . . . Tsigaridis, K. (2018). The Response of the Ozone Layer to Quadrupled CO2 Concentrations. *Journal of Climate, 31*(10), 3893-3907. doi:10.1175/jcli-d-17-0492.1

Crutzen, P. J., & Brühl, C. (1993). A model study of atmospheric temperatures and the concentrations of ozone, hydroxyl, and some other photochemically active gases during the glacial, the pre-industrial Holocene and the present. *Geophysical Research Letters, 20*(11), 1047-1050. doi:10.1029/93GL01423

Danabasoglu, G., Lamarque, J.-F., Bacmeister, J., Bailey, D. A., DuVivier, A. K., Edwards, J., . . . Strand, W. G. (2020). The Community Earth System Model Version 2 (CESM2). *Journal of Advances in Modeling Earth Systems, 12*(2), e2019MS001916. doi:10.1029/2019ms001916

Dietmüller, S., Ponater, M., & Sausen, R. (2014). Interactive ozone induces a negative feedback in CO2-driven climate change simulations. *Journal of Geophysical Research: Atmospheres, 119*(4), 1796-1805. doi:10.1002/2013JD020575

Fu, Q., White, R. H., Wang, M., Alexander, B., Solomon, S., Gettelman, A., . . . Lin, P. (2020). The Brewer-Dobson Circulation During the Last Glacial Maximum. *Geophysical Research Letters, 47*(5), e2019GL086271. doi:10.1029/2019GL086271

Garcia, R. R., Marsh, D. R., Kinnison, D. E., Boville, B. A., & Sassi, F. (2007). Simulation of secular trends in the middle atmosphere, 1950–2003. *Journal of Geophysical Research: Atmospheres, 112*(D9). doi:10.1029/2006JD007485

Garcia, R. R., & Randel, W. J. (2008). Acceleration of the Brewer–Dobson Circulation due to Increases in Greenhouse Gases. *Journal of the Atmospheric Sciences, 65*(8), 2731-2739. doi:10.1175/2008JAS2712.1

Garcia, R. R., Randel, W. J., & Kinnison, D. E. (2011). On the Determination of Age of Air Trends from Atmospheric Trace Species. *Journal of the Atmospheric Sciences, 68*(1), 139-154. doi:10.1175/2010JAS3527.1

Geng, L., Murray, L. T., Mickley, L. J., Lin, P., Fu, Q., Schauer, A. J., & Alexander, B. (2017). Isotopic evidence of multiple controls on atmospheric oxidants over climate transitions. *Nature, 546*(7656), 133-136. doi:10.1038/nature22340

Gettelman, A., Mills, M. J., Kinnison, D. E., Garcia, R. R., Smith, A. K., Marsh, D. R., . . . Randel, W. J. (2019). The Whole Atmosphere Community Climate Model Version 6 (WACCM6). *Journal of Geophysical Research: Atmospheres, 124*(23), 12380-12403. doi:10.1029/2019JD030943

Hall, T. M., & Plumb, R. A. (1994). Age as a diagnostic of stratospheric transport. *Journal of Geophysical Research: Atmospheres, 99*(D1), 1059-1070. doi:10.1029/93JD03192

Hansen, J., Sato, M., Russell, G., & Kharecha, P. (2013). Climate sensitivity, sea level and atmospheric carbon dioxide. *Philosophical Transactions of the Royal Society A:*

Mathematical, Physical and Engineering Sciences, 371(2001), 20120294. doi:10.1098/rsta.2012.0294

Hardiman, S. C., Andrews, M. B., Andrews, T., Bushell, A. C., Dunstone, N. J., Dyson, H., . . . Wood, R. A. (2019). The Impact of Prescribed Ozone in Climate Projections Run With HadGEM3-GC3.1. *Journal of Advances in Modeling Earth Systems, 11*(11), 3443-3453. doi:10.1029/2019MS001714

Hopcroft, P. O., Valdes, P. J., O'Connor, F. M., Kaplan, J. O., & Beerling, D. J. (2017). Understanding the glacial methane cycle. *Nature Communications, 8*(1), 14383. doi:10.1038/ncomms14383

Joussaume, S., & Taylor, K. (1995). Status of the paleoclimate modeling intercomparison project (PMIP). *World Meteorological Organization-Publications-WMO TD*, 425-430.

Kageyama, M., Harrison, S. P., Kapsch, M. L., Lofverstrom, M., Lora, J. M., Mikolajewicz, U., . . . Zhu, J. (2021). The PMIP4 Last Glacial Maximum experiments: preliminary results and comparison with the PMIP3 simulations. *Clim. Past, 17*(3), 1065-1089. doi:10.5194/cp-17-1065-2021

Lorius, C., Jouzel, J., Raynaud, D., Hansen, J., & Treut, H. L. (1990). The ice-core record: climate sensitivity and future greenhouse warming. *Nature, 347*(6289), 139-145. doi:10.1038/347139a0

Marsh, D. R., Lamarque, J.-F., Conley, A. J., & Polvani, L. M. (2016). Stratospheric ozone chemistry feedbacks are not critical for the determination of climate sensitivity in CESM1(WACCM). *Geophysical Research Letters, 43*(8), 3928-3934. doi:10.1002/2016GL068344

Martinerie, P., Brasseur, G. P., & Granier, C. (1995). The chemical composition of ancient atmospheres: A model study constrained by ice core data. *Journal of Geophysical Research: Atmospheres, 100*(D7), 14291-14304. doi:10.1029/95JD00826

Mills, M. J., Schmidt, A., Easter, R., Solomon, S., Kinnison, D. E., Ghan, S. J., . . . Gettelman, A. (2016). Global volcanic aerosol properties derived from emissions, 1990–2014, using CESM1(WACCM). *Journal of Geophysical Research: Atmospheres, 121*(5), 2332-2348. doi:10.1002/2015JD024290

Murray, L. T., Mickley, L. J., Kaplan, J. O., Sofen, E. D., Pfeiffer, M., & Alexander, B. (2014). Factors controlling variability in the oxidative capacity of the troposphere since the Last Glacial Maximum. *Atmos. Chem. Phys., 14*(7), 3589-3622. doi:10.5194/acp-14-3589-2014

Muthers, S., Anet, J. G., Stenke, A., Raible, C. C., Rozanov, E., Brönnimann, S., . . . Schmutz, W. (2014). The coupled atmosphere–chemistry–ocean model SOCOL-MPIOM. *Geosci. Model Dev., 7*(5), 2157-2179. doi:10.5194/gmd-7-2157-2014

Neale, R. B., Chen, C.-C., Gettelman, A., Lauritzen, P. H., Park, S., Williamson, D. L., . . . Lamarque, J.-F. (2010). Description of the NCAR community atmosphere model (CAM 5.0). *NCAR Tech. Note NCAR/TN-486+ STR, 1*(1), 1-12. Retrieved from https://www.cesm.ucar.edu/models/cesm1.0/cam/docs/description/cam5_desc.pdf

Noda, S., Kodera, K., Adachi, Y., Deushi, M., Kitoh, A., Mizuta, R., . . . Yoden, S. (2018). Mitigation of Global Cooling by Stratospheric Chemistry Feedbacks in a Simulation of the Last Glacial Maximum. *Journal of Geophysical Research: Atmospheres, 123*(17), 9378-9390. doi:10.1029/2017JD028017

Nowack, P. J., Luke Abraham, N., Maycock, A. C., Braesicke, P., Gregory, J. M., Joshi, M. M., . . . Pyle, J. A. (2015). A large ozone-circulation feedback and its implications for global warming assessments. *Nature Climate Change, 5*(1), 41-45. doi:10.1038/nclimate2451

Otto-Bliesner, B. L., Brady, E. C., Clauzet, G., Tomas, R., Levis, S., & Kothavala, Z. (2006). Last glacial maximum and Holocene climate in CCSM3. *Journal of Climate, 19*(11), 2526-2544. doi:10.1175/JCLI3748.1

Power, M. J., Marlon, J., Ortiz, N., Bartlein, P. J., Harrison, S. P., Mayle, F. E., . . . Zhang, J. H. (2008). Changes in fire regimes since the Last Glacial Maximum: an assessment based on a global synthesis and analysis of charcoal data. *Climate Dynamics, 30*(7), 887-907. doi:10.1007/s00382-007-0334-x

Rind, D., Lerner, J., McLinden, C., & Perlwitz, J. (2009). Stratospheric ozone during the Last Glacial Maximum. *Geophysical Research Letters, 36*(9). doi:10.1029/2009GL037617

Sherwood, S. C., Webb, M. J., Annan, J. D., Armour, K. C., Forster, P. M., Hargreaves, J. C., . . . Zelinka, M. D. (2020). An assessment of Earth's climate sensitivity using multiple lines of evidence. *Reviews of Geophysics, n/a*(n/a), e2019RG000678. doi:10.1029/2019RG000678

Solomon, S., Rosenlof, K. H., Portmann, R. W., Daniel, J. S., Davis, S. M., Sanford, T. J., & Plattner, G.-K. (2010). Contributions of Stratospheric Water Vapor to Decadal Changes in the Rate of Global Warming. *Science, 327*(5970), 1219-1223. doi:doi:10.1126/science.1182488

Tierney, J. E., Zhu, J., King, J., Malevich, S. B., Hakim, G. J., & Poulsen, C. J. (2020). Glacial cooling and climate sensitivity revisited. *Nature, 584*(7822), 569-573. doi:10.1038/s41586-020-2617-x

Wang, M., Fu, Q., Solomon, S., White, R. H., & Alexander, B. (2020). Stratospheric Ozone in the Last Glacial Maximum. *Journal of Geophysical Research: Atmospheres, 125*(21), e2020JD032929. doi:10.1029/2020JD032929

Zhu, J., Otto-Bliesner, B. L., Brady, E. C., Gettelman, A., Bacmeister, J. T., Neale, R. B., . . . Kay, J. E. (2022). LGM paleoclimate constraints inform cloud parameterizations and equilibrium climate sensitivity in CESM2. *Journal of Advances in Modeling Earth Systems, n/a*(n/a), e2021MS002776. doi:10.1029/2021MS002776

Zhu, J., Otto-Bliesner, B. L., Brady, E. C., Poulsen, C. J., Tierney, J. E., Lofverstrom, M., & DiNezio, P. (2021). Assessment of Equilibrium Climate Sensitivity of the Community Earth System Model Version 2 Through Simulation of the Last Glacial Maximum. *Geophysical Research Letters, 48*(3), e2020GL091220. doi:10.1029/2020GL091220

Zhu, J., & Poulsen, C. J. (2021). Last Glacial Maximum (LGM) climate forcing and ocean dynamical feedback and their implications for estimating climate sensitivity. *Clim. Past, 17*(1), 253-267. doi:10.5194/cp-17-253-2021

Zhu, J., Poulsen, C. J., & Otto-Bliesner, B. L. (2020). High climate sensitivity in CMIP6 model not supported by paleoclimate. *Nature Climate Change, 10*(5), 378-379. doi:10.1038/s41558-020-0764-6

Table 1. The coupled CESM2 simulations of the preindustrial (PI) and Last Glacial Maximum (LGM) with a high-top WACCM6ma (HghTop) and a low-top CAM6 (LowTop) atmosphere component model. Listed are simulation name, boundary conditions of greenhouse gas (GHG), land ice sheet (LIS), orbital parameters, and aerosol emissions, simulation length (years), and mean and standard deviation of global mean surface temperature (GMST; °C) and top-of-atmosphere radiation imbalance (N; W m^{-2}). Average and the standard deviation of GMST and N are derived from the last 70 years of each simulation. LGM_HghTopA uses altered aerosol emissions based on the preindustrial with the anthropogenic emissions removed, fire emissions of CO and NOx scaled by 10%, and soil NOx emission scaled by 98%. See text for details.

Name	GHG, LIS, orbital	Aerosol emission	Length	GMST	N
PI_LowTop	PI	PI	500	13.94±0.10	0.04±0.54
LGM_LowTop	21 ka	PI	500	7.12±0.09	–0.11±0.46
PI_HghTop	PI	PI	300	13.99±0.10	0.07±0.46
LGM_HghTop	21 ka	PI	300	6.96±0.10	–0.10±0.47
LGM_HghTopA	21 ka	Altered	100	6.91±0.10	–0.10±0.43

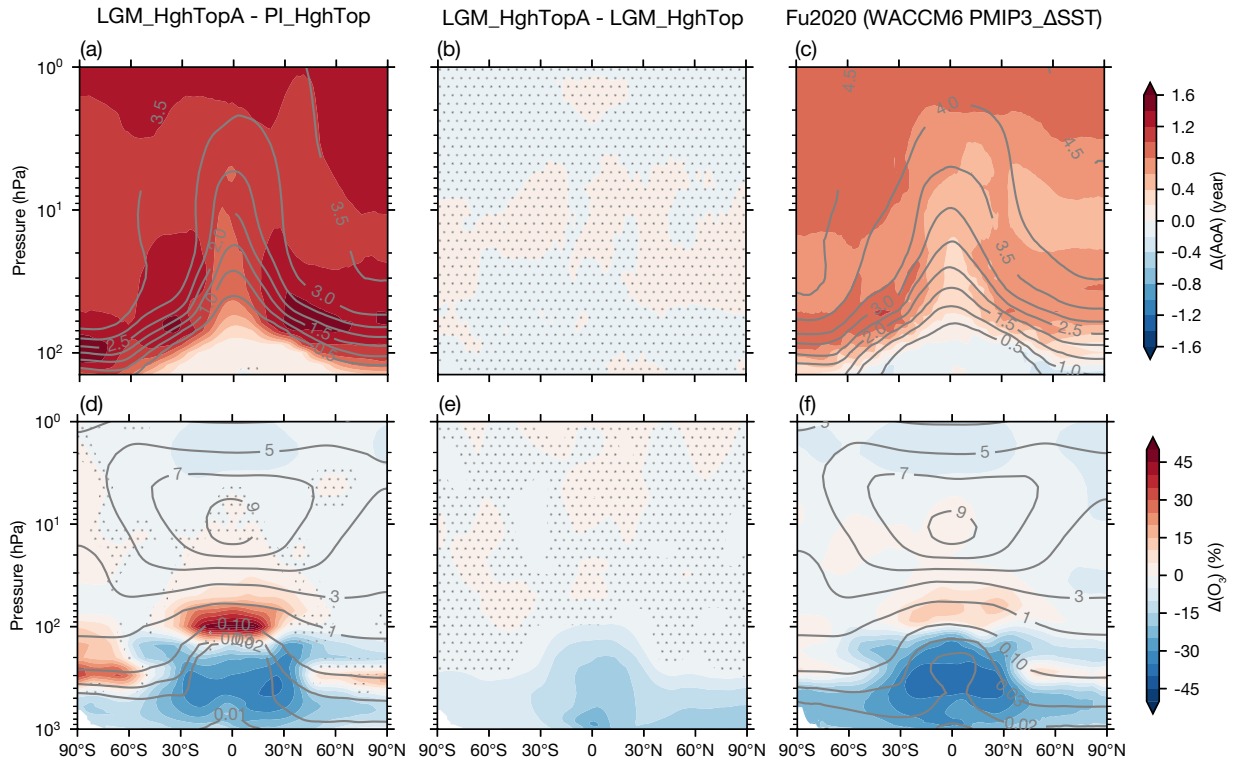

Figure 1. (**a**) Changes in the zonal mean age of stratospheric air (AoA; shadings) between LGM_HghTopA and PI_HghTop. (**b**) Differences in AoA between LGH_HghTopA and LGM_HghTop, showing the sensitivity to the treatment of LGM aerosol emissions. (**c**) LGM AoA changes (shadings) in the WACCM6 atmosphere-only simulations (Fu et al., 2021). (**d**)–(**f**), the same as (**a**)–(**c**) but for ozone change in percentage of the preindustrial values. Contours in (**a**), (**c**), (**d**), and (**f**) show the AoA and ozone (units: ppmv) in the corresponding preindustrial simulations. Note the uneven contour interval in (**d**) and (**f**). Stippling indicates that the differences are not significant at 95% confidence level based on Student's t-test.

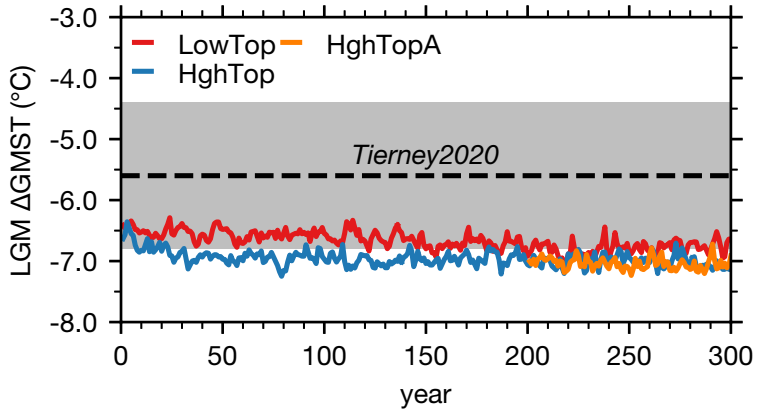

447

448 **Figure 2.** Time series of the global mean surface temperature difference (ΔGMST) between the
449 paired LGM and PI simulations: LowTop = LGM_LowTop – PI_LowTop, HghTop =
450 LGM_HghTop – PI_HghTop, and HghTopA = LGM_HghTopA – PI_HghTop. Black dashed line
451 with the gray patch denotes the 95% uncertainty interval from Tierney et al. (2020) for the LGM
452 ΔGMST. See Table 1 and text for description of the simulations.

453

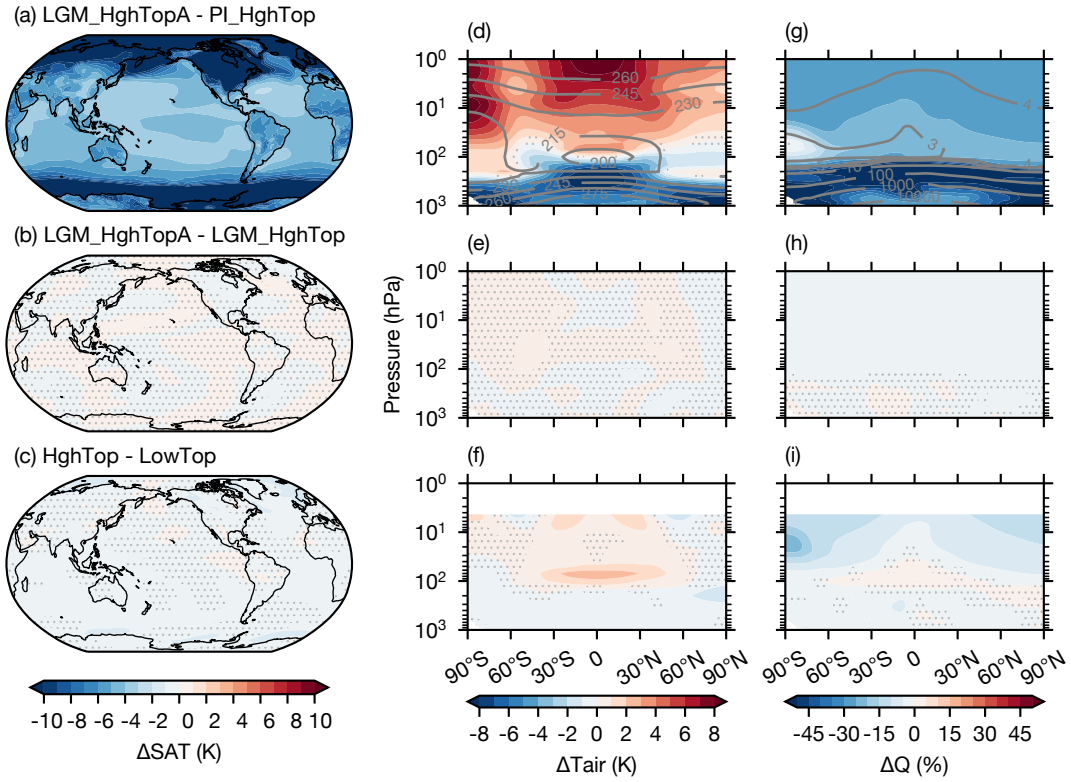

Figure 3. (**a**) Changes in the surface air temperature (SAT) between LGM_HghTopA and PI_HghTop. (**b**) Differences in SAT between LGH_HghTopA and LGM_HghTop, showing the sensitivity to the treatment of LGM aerosol emissions. (**c**) Differences in LGM ΔSAT between high-top and low-top simulations, showing the sensitivity to stratospheric dynamics and chemistry. (**d**)–(**f**), the same as (**a**)–(**c**) but for the zonal mean of air temperature. (**g**)–(**i**), the same as (**a**)–(**c**) but for the zonal mean of water vapor in percentage of the preindustrial values. Contours in (**d**) and (**g**) show the zonal mean SAT and water vapor mixing ratio (units: ppmv) in the corresponding preindustrial simulations. Note the uneven contour interval in (**g**). Stippling indicates that the differences are not significant at 95% confidence level based on Student's t-test.